Published in final edited form as:

Clin Cancer Res. 2019 October 01; 25(19): 5984–5996. doi:10.1158/1078-0432.CCR-18-3399.

Dual farnesyl and geranylgeranyl transferase inhibitor thwarts mutant KRAS-driven patient-derived pancreatic tumors

Aslamuzzaman Kazi[1,2], **Shengyan Xiang**[1], **Hua Yang**[1], **Liwei Chen**[1], **Perry Kennedy**[1], **Ayaz Mohamed**[1,3], **Steven Fletcher**[4], **Christopher Cummings**[5], **Harshani Lawrence**[1,2,3], **Francisca Beato**[6], **Ya'an Kang**[7], **Michael P. Kim**[7], **Andrea Delitto**[8], **Patrick Underwood**[8], **Jason B. Fleming**[6], **Jose Trevino**[8], **Andrew D. Hamilton**[5], **Said M. Sebti**[1,2,3]

[1]Drug Discovery Department, H. Lee Moffitt Cancer Center and Research Institute, Tampa, Florida;

[2]Department of Oncologic Sciences, University of South Florida, Tampa, Florida;

[3]Chemical Biology Core Facility, H. Lee Moffitt Cancer Center and Research Institute, Tampa, Florida;

[4]University of Toronto, Ontario, Canada;

[5]Department of Chemistry, Yale University, New Haven, Connecticut;

[6]Department of Gastrointestinal Oncology, H. Lee Moffitt Cancer Center and Research Institute, Tampa, Florida;

[7]Department of Surgical Oncology, University of Texas MD Anderson Cancer Center, Houston, Texas;

[8]Department of Surgery, University of Florida, Gainesville, Florida;

Abstract

Purpose: Mutant KRAS is a major driver of pancreatic oncogenesis and therapy resistance, yet KRAS inhibitors are lacking in the clinic. KRAS requires farnesylation for membrane localization and cancer-causing activity prompting the development of farnesyltransferase inhibitors (FTIs) as anti-cancer agents. However, KRAS becomes geranylgeranylated and active when cancer cells are treated with FTIs. To overcome this geranylgeranylation-dependent resistance to FTIs, we designed FGTI-2734, a RAS C-terminal mimetic dual FT and geranylgeranyltransferase-1 inhibitor (GGTI).

Current address of Andrew D. Hamilton: New York University, New York, NY.

Current address of Said Sebti: Massey Cancer Center, Virginia Commonwealth University, Richmond, Virginia.

Author contributions

A.K., S.X., H.Y., L.C., P.K., FB, and YK performed experiments, collected data, and prepared the figures. A.M., H.L., S.F., and C.C. synthesized, purified, and characterized the compounds. J.T., J.F., and M.K. generated IRB-approved harvest of resected fresh tumor biopsies from pancreatic cancer patients. P.U. collected data. A.D. performed mutational analysis. A.D.H. supervised the chemical synthesis of the compounds. S.M.S. designed experiments, supervised the work, and wrote the manuscript. All authors reviewed the manuscript.

Conflict of interest: Said Sebti and Andrew Hamilton are co-inventors of GGTI-2418, FTI-2148, and FGTI-2734. Said Sebti is chief scientific officer of Prescient Therapeutics who has the license to GGTI-2418.

Experimental Design: Immunofluorescence, cellular fractionation, and gel shift assays were used to assess RAS membrane association, western blotting to evaluate FGTI-2734 effects on signaling and mouse models to demonstrate its antitumor activity.

Results: FGTI-2734, but not the selective FTI-2148 and GGTI-2418, inhibited membrane localization of KRAS in pancreatic, lung, and colon human cancer cells. FGTI-2734 induced apoptosis and inhibited the growth in mice of mutant KRAS-dependent but not mutant KRAS-independent human tumors. Importantly, FGTI-2734 inhibited the growth of xenografts derived from four pancreatic cancer patients with mutant KRAS (two G12D, two G12V) tumors. FGTI-2734 was also highly effective at inhibiting, in three-dimensional co-cultures with resistance-promoting pancreatic stellate cells, the viability of primary and metastatic mutant KRAS tumor cells derived from 8 pancreatic cancer patients. Finally, FGTI-2734 suppressed oncogenic pathways mediated by AKT, mTOR, and cMYC while upregulating p53 and inducing apoptosis in patient-derived xenografts in vivo.

Conclusion: The development of this novel dual FGTI overcomes a major hurdle in KRAS resistance, thwarting growth of patient-derived mutant KRAS-driven xenografts from pancreatic cancer patients, and as such it warrants further preclinical and clinical studies.

Members of the RAS family of GTPases are signal transducers that regulate many biological processes, including cell cycle progression, cell survival, and differentiation (1–3). When mutated, they become persistently activated and promote several oncogenic events, including uncontrolled proliferation, resistance to apoptosis, sustained angiogenesis, invasion, and metastasis (1). Approximately 20% to 30% of all solid tumors have mutations in the KRAS, NRAS, or HRAS isoforms (1–3). Among these three RAS isoforms, oncogenic mutant KRAS is associated with currently unsolved lethality of several solid tumor neoplasms, particularly where it is prevalent such as in 90% of pancreatic, 45% of colorectal, and 35% of lung carcinomas (4–7). For example, patients whose tumors harbor mutant KRAS respond poorly to chemotherapy and targeted therapies, have poor prognosis, and have more aggressive tumors (4–7). The United States National Cancer Institute identified the targeting of KRAS as a high priority and has implemented several major initiatives with the ultimate goal of discovering therapies that specifically target patients whose tumors harbor mutant KRAS. However, targeting KRAS directly is challenging (8–12). Although recent efforts have led to encouraging results (10–12), no anti-cancer drugs targeting mutant KRAS are available in the clinic. Therefore, indirect and alternative approaches to targeting mutant KRAS human tumors are greatly needed.

One alternative approach is to inhibit KRAS prenylation, a lipid post-translational modification that is required for the proper cellular localization and cancer-causing activity of KRAS (13). The two enzymes involved in KRAS prenylation are farnesyltransferase (FT) and geranylgeranyltransferase 1 (GGT-1), which transfer farnesyl and geranylgeranyl lipids to the cysteine sulfhydryl of proteins terminating at their carboxyl terminal with CAAX tetrapeptide sequences (where C = cysteine, A = aliphatic residues, and X = any amino acid). Farnesyltransferase prefers methionine or serine at the X position, whereas GGT-1 prefers a leucine or isoleucine at the X position (13). The fact that KRAS and other GTPases require prenylation for their ability to induce malignant transformation has led to the development of FT inhibitors (FTIs) and GGT-1 inhibitors (GGTIs) as potential anti-cancer

agents(13). All RAS isoforms are exclusively farnesylated. However, when cells are treated with FTIs, KRAS and NRAS, but not HRAS, become geranylgeranylated by GGT-1, and the resulting geranylgeranylated KRAS and NRAS are fully functional[13]. Blocking FT is sufficient to inhibit HRAS, but blocking both FT and GGT-1 is required to inhibit the prenylation and function of KRAS and NRAS (13). Therefore, a single molecule with dual inhibitory activities has the potential to abrogate mutant KRAS- and mutant NRAS-driven human cancers.

Pancreatic cancer is the fourth leading cause of cancer-related deaths in the United States, with less than 6% of patients surviving 5 years following diagnosis (14, 15). The persistently poor survival rate of pancreatic cancer patients is due to resistance to current treatments, with mutant KRAS (> 90% prevalence) as a major contributor (14). In this study, we describe the development of FGTI-2734, a potent CAAX tetrapeptide mimetic dual FT and GGT-1 inhibitor that prevented KRAS membrane localization and inhibited the in vivo growth of several mutant KRAS-driven human cancer cells and growth of patient-derived xenografts (PDXs) from mutant KRAS tumors from 4 pancreatic cancer patients. Using three-dimensional co-cultures with chemoresistance-promoting pancreatic stellate cells, we found that FGTI-2734 inhibited the growth and viability of primary and metastatic mutant KRAS tumor cells derived from pancreatic cancer patients. Importantly, FGTI-2734 suppressed major cancer-causing pathways (i.e., PI3K/AKT/mTOR and cMYC) while upregulating the tumor suppressor p53 and inducing apoptosis in patient-derived xenografts in vivo.

Methods

Cells lines, cell culture, and reagents

Human lung cancer cell lines (A549, H460 and Calu6), colon cancer cell line (DLD1), and pancreatic cancer cell lines (MiaPaCa2, L3.6pl) were obtained from the ATCC (Manassas, VA, USA). Human lung cancer cell lines H522, H661, H322, H2126, and normal lung fibroblast cell lines WI-38 and MRC-5 were kindly provided by Dr. Eric Haura (Moffitt Cancer Center, Tampa, FL, USA). NIH3T3 cells stably transfected with constitutively active H-Ras61L (H-Ras/NIH3T3), K-RasGV12 (K-Ras/NIH3T3), N-Ras (N-Ras/NIH3T3), and empty vector pcDNA3 (pcDNA3/NIH3T3) were obtained from Dr. Channing Der (University of North Carolina, Chapel Hill, NC, USA). Normal fibroblast cells WI-38 and MRC-5 were cultured in MEM, and all other cell lines were cultured in Dulbecco's modified eagle's medium or RPMI-1640 medium. All media were supplemented with 10% heat-inactivated fetal bovine serum (FBS), 10 U/mL penicillin, and 10 μg/mL streptomycin. All cell lines were mycoplasma-free, monitored regularly with HEK-blue2 cells and mycoplasma detection kit from invivogen (cat# rep-pt1). All cell lines were authenticated by University of Arizona Genetics Core. FGTI-2734, FTI-2148, and GGTI-2418 were synthesized in-house as described previously (16, 17, 35). The FGTI-2734 and FTI-2148 were derivatized as mono-mesylate salt and bistrifluoroacetate salts, respectively.

Human pancreatic cancer cell lines were derived from eight patient pancreatic tumors using IRB-approved (MDA Cancer Center protocol LAB07–0854) and previously described methods (23, 30). The investigators obtained written consent from the subjects. The research

was conducted according to Declaration of Helsinki. The cells were plated at 3000/well in triplicate in a 96-well flat-bottom plate in RPMI medium with 10% FBS. Cells were subsequently treated for 72 hours with DMSO or FGTI-2734 at 3, 10, 30, and 100 μM. For three-dimensional cultures, 15 mL of cold Matrigel growth factor-reduced, phenol red-free solution was added to wells, spread evenly, and allowed to incubate at 37°C for 30 minutes to solidify. Pancreatic cancer cells (3000/well) were resuspended in RPMI-2% Matrigel medium-10% FBS overlaid on the solidified Matrigel and cultured for 24 hours before treatment. For three-dimensional co-culture with pancreatic stellate cells, human pancreatic stellate cells were grown until confluent in RPMI with 10% FBS. Matrigel was added as in 3D culture and pancreatic cancer cells and human pancreatic stellate cells were resuspended at 3000 cells/well in RPMI-2% Matrigel medium supplemented with 10% FBS, overlaid at 1:1 ratio, and cultured for 24 hours before treatment.

In vitro FT and GGT-1 activity assays

GGT-1 and FT activities from 60,000*g* supernatants of human Burkitt lymphoma (Daudi) cells (obtained from ATCC) were assayed as described previously (17). We conducted tests to determine the ability of peptidomimetics to inhibit the transfer of [^{3}H]geranylgeranyl and [^{3}H]farnesyl from [^{3}H]geranylgeranylpyrophosphate (Perkin-Elmer, Wellesley, MA, USA) and from [^{3}H]farnesylpyrophosphate (Amersham Biosciences, Piscataway, NJ) to recombinant HRAS-CVLL and HRAS-CVLS, respectively.

Western blot analysis

To prepare whole cell lysates, cells were trypsinized, washed twice with cold phosphate-buffered saline (PBS), and lysed in mammalian protein extraction reagent (product no. 78501, Thermo Fisher Scientific, Rockford, IL, USA) supplemented with protease inhibitor cocktail (product no. A32953, Thermo Fisher Scientific), consisting of 2 mM phenylmethylsulfonyl fluoride, 2 mM Na_3VO_4, and 6.4 mg/mL *p*-nitrophenylphosphate. Tumor tissue samples were lysed in tissue protein extraction reagent (product no. 78510, Thermo Fisher Scientific) with above supplements. The automatic hand-operated OMNI-TIP homogenizer (Omni International, Inc. Kennesaw, GA, USA) was used to homogenize the tumor tissues. Lysates from whole cells and tumor homogenates were cleared by centrifugation at 12,000*g* for 15 minutes, and the supernatants were collected as whole cell extracts. Protein concentrations were determined using the BCA protein assay kit. Proteins were separated by SDS-PAGE and transferred to nitrocellulose membranes (17), which were then blotted with antibodies specific for unprenylated RAP1A (catalog no. sc-1482), HRAS (no. sc-520), NRAS (no. sc-519), IGF-1Rβ (3G5C1; no. sc-81167), AKT1/2 (N-19; no. sc-1619), p53 (DO-1; no. sc-126), and cMYC (pE10; no. sc-40) (all from Santa Cruz Biotechnology, Santa Cruz, CA, USA). Other antibodies included phospho-AKT (S473; catalog no.9271S), phospho-ERK (no. 9101L), ERK (no. 9102L), cleaved-CASP-3 (no. 9664L), cleaved-PARP (no. 5625S), phospho-S6 ribosomal protein (no. 2215S), and S6 ribosomal protein (no. 2217S) from Cell Signaling (Danvers, MA, USA); RHOGDI/D4-GDI (no. 66586E) from BD Pharmingen (San Jose, CA, USA); anti-c-KRAS (Ab-1; no. OP24) from Calbiochem (Millipore, Billerica, MA, USA); HDJ-2 from Lab Vision Corporation (Fremont, CA, USA); and anti-β-ACTIN (no A5441-.2ML) and vinculin (no. V9131-.2ML) from Sigma-Aldrich (St. Louis, MO, USA).

Membrane and cytosol fractionation

Membrane and cytosolic fractions were prepared according to van der Hoeven et al (36) Briefly, cells were grown in 10-cm dishes, treated for 72 hours with drugs (FGTI, FTI, and GGTI) or vehicle control (DMSO), and washed twice with cold PBS. Cells were then harvested by scraping into fractionation buffer (10 mM Tris [pH 7.5], 25 mM NaF, 5 mM $MgCl_2$, 1 mM EGTA, 1 mM dithiothreitol, 100 μM Na_3VO_4 plus protease inhibitors), incubated on ice for 30 minutes, and lysed by passing through a 23-gauge needle 26 times. Lysed cells were then centrifuged at 1000*g* for 5 minutes at 4°C to remove nuclear fractions and unbroken cells, with supernatants then centrifuged at 100,000*g* at 4°C for 30 minutes in a refrigerated ultracentrifuge (Optima Max Ultracentrifuge, Beckman Coulter, Fullerton, CA, USA) to sediment plasma membranes. The cytosolic supernatant (S100) was separated from the membrane pellet. The crude membrane pellet was washed once (without disturbing the pellet) with the above fractionation buffer and then resuspended in the above buffer by sonication (3× for 30 seconds each) and used as membrane fraction (P100). Protein concentrations of both fractions were determined using BCA protein assay kit, and 15 to 20 μg of both fractionation proteins underwent SDS-PAGE and Western blotting with the specific antibodies.

Vector construction, lentivirus production, and guide RNA-mediated knockout of KRAS

The lentiCRISPRv2 plasmid was a gift from Feng Zhang (Addgene plasmid no 52961). Guide RNAs were designed using the CRISPR design tool (http://crispr.mit.edu). The non-target scramble control (SC) and sgKRAS vectors were generated using Feng Zhang's protocol, which is available on Addgene's website (www.addgene.org). The guide RNA sequences of SC and sgKRAS are 5'-GCACTACCAGAGCTAACTCA-3' and 5'-GCAATGAGGGACCAGTACATG-3', respectively. For lentivirus production, the lentiviral vector (10 μg), pMD.2G (5 μg), and pspPax2 (5 μg) vectors were cotransfected into 293T cells using polyethylenimine (25 kDa, 1 μg/μL). At 48 hours, the virus supernatants were collected and concentrated at 1:100 ratio using the Lenti-X™ concentrator (Clontech, 631231). Cells were transduced overnight using 10 μL of concentrated virus with 8 μg/mL of polybrene and then cultured for an additional 72 hours before harvest and Western Blot analyses.

Immunofluorescence

The immunofluorescence vectors pLEX-GFP, pLEX-GFP-KRASG12V-CVIM, and pLEXGFP-KRASG12V-SVIM were constructed in a modified pLEX-FLAG vector. A GFP sequence was inserted between *Not*I and *Bam*HI sites, and KRAS sequences were inserted after GFP and between *Bam*HI and *Age*I sites. Lentivirus production was carried out as described above. Cells (0.8×10^5) were plated onto glass coverslips in 12-well plates and left overnight, after which the cells were infected with 200×10^8 copies of GFP-KRASG12V with wild-type CAAX box (GFP-KRASG12V-CVIM), GFP-tagged mutated prenylation cysteine 185 to the non-prenylable serine 185 (GFPKRASG12V-SVIM), and corresponding empty vector (GFP-EV). After 24 hours of infection, cells were treated with vehicle control and different concentrations of FGTI-2734, FTI-2148, and GGTI-2418 for 48 hours. Cells were then washed once with warm Dulbecco's PBS (catalog no. 14190–144,

GIBCO Life Technologies, Invitrogen) and fixed with prewarmed 4% paraformaldehyde solution in PBS (no. sc-281692, Santa Cruz Biotechnology) for 5 minutes at room temperature. After fixation, cells were washed 3 times with Dulbecco's PBS, with coverslips mounted using Vectashield with 4',6-diamidino-2-phenylindole (H-1200; Vector Labs, Burlingame, CA, USA). Localization of GFP was observed using a confocal microscope (×40 magnification).

Cell viability assay and live cell imaging

Cell viability was determined by the CellTiter-Glo luminescent cell viability assay (Promega, Madison, WI, USA) according to the manufacturer's protocol. Briefly, cells (10^3 cells/well) were seeded in 384-well plates, allowed to adhere overnight, and treated with vehicle (DMSO) or drugs for 72 hours, after which they were processed for viability using CellTiter-Glo reagent. Data were normalized to percentage of control, and IC50 values were determined. Each condition was performed in replicates of 6 wells. For the patient-derived cells, IC50 was calculated using GraphPad Prism 7.02 software. Live-cell imaging was carried out with the IncuCyte ZOOM. Wells were scanned at day 0 and at 72 hours of treatment. Cell number was determined using IncuCyte software, and day 0 scan was used as control.

Antitumor studies of human tumor xenografts in mice

Male SCID-bg mice (Charles River Laboratories, Wilmington, MA, USA) were maintained and treated in accordance with our Institutional Animal Care and Use Committee procedures and guidelines. Exponentially growing MiaPaCa2, L3.6pl, Calu6, A549, DLD1, and H460 cells were harvested via trypsinization, pelleted at 300*g* for 5 minutes, resuspended in sterile Dulbecco's PBS (Invitrogen) at 10×10^6 cells (L3.6pl and A549), 5×10^6 cells (MiaPaCa2, Calu6, and DLD1), and 3×10^6 cells (H460) per 100 μL, and injected into the flank of each mouse. The tumor xenografts were monitored 3 days/week with an electronic caliper. Tumor volume was calculated using the formula $V = (L^2 W)/2$, where L is length and W is width, with width defined as the largest measurement and length as the smallest measurement. When the tumors reached approximately 200 mm^3, the animals were randomized to the following treatment groups: (1) vehicle control group (40% 2-hydroxypropyl-β-cyclodextrin [Sigma] wt/vol in sterile water), administered once daily via 100-μL intraperitoneal injections, and (2) FGTI-2734 group, with FGTI-2734 administered at 100 mg/kg/daily intraperitoneally in 40% 2-hydroxypropyl-β-cyclodextrin. Treatments were continued for 18 to 25 days. For both groups, animals showed no evidence of gross toxicity as measured by weight loss.

Antitumor efficacy studies of patient-derived xenografts of tumors from pancreatic cancer patients

To determine whether pharmacological inhibition of KRAS can inhibit the growth of PDXs, we obtained fresh tumor biopsies from pancreatic cancer patients (University of Florida, IRB protocol 201600873) with KRAS mutation. The investigators obtained written consent from the subjects. The research was conducted according to International Ethical Guidelines for Biomedical Research Involving Human Subjects.

Specifically, fresh 2-mm tumor pieces were obtained from pancreatic resection and transported on ice to the animal surgery suite for subcutaneous implantation into NOD.Cg-Prkdcscid Il2rgtm1Wjl/SzJ (NSG) mice. The mice were housed, maintained, and treated in accordance with our Institutional Animal Care and Use Committee procedures and guidelines. After 1-cm incisions were made on right flanks of anesthetized NSG mice, the subcutaneous layer underwent blunt dissection. A viable tumor piece was then placed, and the skin was closed with surgical clips (generation 1). Once engrafted and tumors reached 1.5 cm in diameter, tumors were divided evenly into 2-mm pieces and reimplanted into NSG mice as above (generation 2). Generation 3 was generated similarly (details as described in Delitto et al, ref. 22). When the tumors of generation 2 or 3 mice reached approximately 100–200 mm^3, the animals were randomized into vehicle and FGTI-2734 treatment groups as described above for the xenograft models.

RAF-1 kinase assay

MiaPaCa 2 cells were treated with vehicle and FGTI-2734 (30 μM) or infected with lentiviral plex-Flag-GFP (EV), plex-Flag-GFP-KRAS (C185) and plex-Flag-GFP-KRAS (S185). Forty-eight hours after treatment or infection, cells were harvested with Cell Lysis Buffer (20 mM Tris (pH 7.5), 150 mM NaCl, 1 mM EDTA, 1 mM EGTA, 0.1%Triton X-100, 2.5 mM sodium pyrophosphate, 1 mM β-glycerophosphate,1 mM Na_3VO_4, 1 μg/ml Leupeptin and 1 mM PMSF). The cell lysates (1.5~2 mg, 1000 μl each) were used for immunoprecipitation with RAF-1 antibody (Santa Cruz, # sc-7267) or anti-Flag M2 affinity gel (Sigma, #A2220) for 3 hours at 4°C. The protein bound beads were washed 2 times with Cell Lysis Buffer and 2 times with kinase buffer (25 mM Tris (pH 7.5), 5 mM β-Glycerolphosphate, 10 mM MgCl2, 1 mM DTT, 0.1 mM Na3VO4). The protein-bound beads were incubated with 40 μl kinase buffer supplemented with 1 μg of inactive MEK1 (Invitrogen, #P3093) and 200 μM ATP (Invitrogen, #AM8110) for 30 minutes at room temperature. The phosphorylated MEK1 was detected by immunoblotting using anti-phospho-MEK1 (Ser217/221) antibody (Cell Signaling Technology, #9121), and total MEK1 detected with anti-MEK1 antibody (Cell Signaling Technology, #9122). For the other immunoblotting, the blots were incubated with antibodies of RAF-1, Flag (Sigma, #F3165), anti-c-k-RAS (Millipore, #OP24), and KSR-1(Santa Cruz, # sc-515924), respectively.

Data availability statement:

All data generated or analysed during this study are included in this published article (and its supplementary information files).

Results

membrane localization in RAS-transformed murine NIH3T3 cells and in mutant KRAS human cancer cells

As shown in Fig. 1A, FTI-2148 inhibited FT and GGT-1 activities in vitro with half-maximal inhibitory concentration (IC50) values of 1.4 nM and 1700 nM, respectively, showing a 1214-fold selectivity for FT over GGT-1. GGTI-2418 inhibited GGT-1 and FT activities in vitro with IC50 values of 9.4 nM and 58,000 nM respectively, demonstrating a 6170-fold selectivity for GGT-1 over FT. In contrast, FGTI-2734 inhibited FT and GGT-1

activities with similar IC50 values of 250 and 520 nM, respectively. This 2-fold difference was not statistically significant (Fig. 1A).

We next evaluated the effects of these 3 inhibitors on RAS membrane association in HRAS-, NRAS-, and KRAS-transformed murine NIH3T3 cells and in human cancer cells harboring mutant KRAS. Western blots in Fig. 1B show that FTI-2148 inhibited the farnesylation of the exclusively farnesylated protein HDJ2 in all 3 RAS-transformed NIH3T3 cells (non-prenylated proteins migrate more slowly than prenylated protein in SDS-PAGE gels (13, 16, 17). In contrast, FTI-2148 did not inhibit the geranylgeranylation of the exclusively geranylgeranylated RAP1A (as documented by an antibody that recognizes only non-geranylgeranylated RAP1A (13, 16, 17), confirming in intact cells the high selectivity in vitro of FTI-2148 for FT over GGT-1 (Fig. 1A). GGTI-2418 inhibited the geranylgeranylation of RAP1A but not the farnesylation of HDJ2 (Fig. 1B), confirming its in vitro selectivity for GGT-1 over FT (Fig. 1A). In contrast, FGTI-2734 inhibited the prenylation of both HDJ2 and RAP1A (Fig. 1B), confirming its in vitro dual FT and GGT-1 inhibitory activity (Fig. 1A). Importantly, FGTI-2734, but not FTI-2148 and GGTI-2418, inhibited the prenylation of KRAS and NRAS (Fig. 1B). As expected, the prenylation of the exclusively farnesylated HRAS was inhibited by FGTI-2734 and FTI-2148 but not by GGTI-2418 (Fig. 1A).

To determine whether FGTI-2734 can inhibit KRAS and NRAS membrane association in human cancer cells, human pancreatic (MiaPaCa2) and lung (H460) cancer cells were treated with the inhibitors and processed for membrane/cytosol cellular fractionations as described in the Methods. As shown in Fig. 1C, FTI-2148 inhibited the membrane association of the farnesylated protein HRAS, leading to its accumulation in the cytosol, but did not affect membrane association and cytosolic accumulation of the geranylgeranylated protein RAP1A. Although GGTI-2418 induced the cytosolic accumulation of non-geranylgeranylated RAP1A, it did not affect membrane association and cytosolic accumulation of HRAS (Fig. 1C). In contrast, FGTI-2734 induced the cytosolic accumulation of both HRAS and RAP1A. Importantly, FGTI-2734, but not FTI-2148 and GGTI-2418, inhibited the membrane association of KRAS and NRAS, which led to the accumulation of these proteins in the cytosol (Fig. 1C, bottom panels).

To determine the effects of the prenylation inhibitors on KRAS cellular localization by immunofluorescence, lentiviruses coding for a GFP-tagged mutant KRAS-G12V with a wild-type C-terminal CAAX box (GFP-KRASG12V-CVIM) and a corresponding empty vector construct (GFP-EV) were generated. We also mutated the cysteine 185 of the CAAX box to serine 185, hence generating a lentivirus coding for GFP-tagged mutant KRASG12V with a mutant CAAX that cannot be prenylated and therefore cannot associate with the membrane (GFP-KRASG12V-SVIM). MiaPaCa2 and H460 cells were infected with the lentiviruses, treated with inhibitors and processed 48 hours after drug treatment for immunofluorescence microscopy as described in the Methods. As shown in Fig. 2A, cells infected with GFP-EV displayed a diffuse pattern of GFP fluorescence. In contrast, cells infected with GFP-KRASG12V-CVIM showed a distinct punctate pattern of primarily plasma membrane localization but also endomembrane, consistent with previous reports (18). As expected, cells infected with GFP-KRASG12V-SVIM showed a diffuse pattern of

GFP fluorescence, confirming the lack of KRAS prenylation and membrane localization (Fig. 2A). FGTI-2734 treatment prevented GFP-KRASG12V-CVIM localization to the membrane, resulting in a diffuse pattern similar to the one observed in the cells infected with the GFP-KRASG12V-SVIM. Importantly, cells treated with FTI-2148 and GGTI-2418 did not prevent GFPKRASG12V-CVIM membrane localization (Fig. 2A). The ability of FGTI-2734 to prevent membrane localization was also demonstrated in other human cancer cell lines, including Calu6, A549, and DLD1 cells (Fig. 2A).

Effects of accumulating KRAS in the cytosol on binding Raf and on Raf kinase activity.

Figures 1C and 2A demonstrated that FGTI-2734 prevents KRAS membrane association and induces accumulation of KRAS in the cytoplasm. We next evaluated the effects of shifting mutant KRAS from the membrane to the cytoplasm by determining whether it is still able to bind one of its major effectors RAF-1, and whether RAF-1 kinase activity is affected. To this end, we treated MiaPaCa2 cells with FGTI-2734 as described above, and processed the cells for RAF-1 immunoprecipitation, followed by immunoblotting of KRAS and KSR, a scaffolding protein that binds RAF-1 and mediates RAS activation of RAF-1. Figure 2B shows that in the absence or presence of FGTI-2734, RAF-1 was able to bind KRAS, suggesting that both membrane and cytosolic KRAS are able to bind RAF-1. However, FGTI-2734 inhibited the binding of RAF-1 to KSR, suggesting that the binding of KSR to RAF-1 requires the membrane environment. To determine the effects of FGTI-2734 on RAF-1 kinase activity, RAF-1 was immunoprecipitated and its kinase activity was assayed in the immunoprecipitates using recombinant inactive MEK1 as a substrate and western blotting with an antibody to phosphorylated Serines 217 and 221, two RAF-1 phosphorylation sites on MEK1. Figure 2B shows that FGTI-2734 inhibited RAF-1 kinase activity suggesting that though cytosolic KRAS binds RAF-1, it requires KSR and the membrane environment to fully activate RAF-1. We next determined whether RAF-1 binds KRASG12V-SVIM, the CAAX mutant that cannot be prenylated and that does not bind to the membrane (see Figure 2A). To this end, we infected MiaPaCa2 cells with lentiviral FLAG-tagged KRASG12V-CVIM and its non-membrane bound mutant FLAG-tagged KRASG12VSVIM, and processed the cells for co-immunoprecipitation and RAF-1 kinase assays. Figure 2C shows that the KRASG12V-SVIM mutant is still able to bind RAF-1 and that the RAF-1 kinase activity in this cytosolic complex is inhibited, confirming the FGTI-2734 results of Figure 2B.

FGTI-2734 induces apoptosis in mutant KRAS-dependent, but not mutant KRAS–independent, human cancer cells

We next determined whether blocking KRAS prenylation with FGTI-2734 can induce apoptosis in human cancer cells that harbor mutant KRAS and whether human cancer cells that depend on mutant KRAS for survival are more sensitive to FGTI-2734. To this end, we first constructed KRAS and scrambled guide RNAs (gRNAs) in LentiCRISPR vectors, and determined whether the viability of 6 human cancer cell lines depends on KRAS by CRISPR/Cas9-targeted knock out of KRAS. As shown in Fig. 3, KRAS gRNA led to KRAS knockout in all cell lines evaluated, including MiaPaCa2 and L3.6pl (pancreatic), Calu6,

A549, and H460 (lung), and DLD1 (colon). Although all 6 cell lines harbor mutant KRAS, KRAS knockout only resulted in apoptosis (as determined by CASPASE-3 and PARP cleavage) in MiaPaCa2, L3.6pl, and Calu6 cells (Fig. 3A) but not in A549, H460, and DLD1 cells (Fig. 3B). Therefore, only MiaPaCa2, L3.6pl, and Calu6 cells depended on KRAS for survival, consistent with previously published studies by us (19) and others (20, 21). Treatment with FGTI-2734 inhibited the farnesylation of HDJ2 and the geranylgeranylation of RAP1A in all 6 cell lines (Fig. 3). However, FGTI-2734 treatment only induced CASPASE-3 and PARP cleavage in MiaPaCa2, L3.6pl, and Calu6 cells (Figs. 3A) but not in A549, H460, and DLD1 cells (Figs. 3B), indicating that FGTI-2734 induces apoptosis only in the three cancer cell lines that are dependent on mutant KRAS for viability. Furthermore, FGTI-2734 did not induce apoptosis in wild-type RAS human cancer cells, including H2126, H522, H661, and H322 lung cancer cells (Supplementary Fig. 1). Finally, FGTI-2734 did not induce apoptosis in normal lung fibroblasts, as shown in the WI-38 and MRC-5 cell lines (Supplementary Fig. 1).

FGTI-2734 inhibits the in vivo growth of mutant KRAS-dependent but not mutant KRAS–independent human tumors in mouse xenograft models

As detailed in the Methods, MiaPaCa2, L3.6pl, Calu6, A549, H460, and DLD1 were subcutaneously implanted in mice; after tumors reached an average size of ~200 mm^3, mice were randomized and treated daily with vehicle or 100 mg/kg body weight FGTI-2734 intraperitoneally. As shown in Figure 4, growth of mutant KRAS-dependent MiaPaCa2 tumors from mice treated with FGTI-2734 was significantly inhibited as early as 2 days after initiation of treatment and continued to be significantly inhibited for the rest of the treatment period. Mice displayed no gross toxicity (no effects on mouse weight, food intake, or activity). Compared with MiaPaCa2 tumors from vehicle control-treated mice, which grew from an average of 224 ± 50 to 1015 ± 235 mm^3, tumor growth in FGTI-2734-treated mice was nearly suppressed, growing from 218 ± 22 to only 302 ± 46 mm^3 (Fig. 4, top left). Similar results were obtained with the other two mutant KRAS-dependent tumors (L3.6pl and Calu6) (Fig. 4, middle and lower left panels). For the mutant KRAS-independent tumors (A549, H460, and DLD-1), FGTI-2734 had no effect on growth (Fig. 4, middle panels). Thus, although all 6 cell tumors harbor mutant KRAS, FGTI-2734 only inhibited tumor growth in mutant KRAS-dependent tumors but not in mutant KRAS-independent tumors.

FGTI-2734 inhibits the growth of mutant KRAS patient-derived xenografts from pancreatic cancer patients

For the rest of the manuscript, we focused on evaluating FGTI-2734 in clinically relevant models using human tumors harvested from patients with pancreatic cancer, as these tumors are known to be driven by mutant KRAS. To this end, we examined the effects of FGTI-2734 on the growth of PDX in mice from four pancreatic cancer patients. Patient 1: T3N1 ductal adenocarcinoma with G12V mutant KRAS, moderately differentiated, 2/17 LN, +LV/PN invasion, 7.8 cm; was refractory to adjuvant gemcitabine and 5FU. Patient 2: T3N1 ductal adenocarcinoma with G12D mutant KRAS, well differentiated, 4/11 LN, +LV,PN invasion, 3.0 cm; had received treatment with adjuvant gemcitabine. Patient 3: T3N0 ductal adenocarcinoma with G12D mutant KRAS, moderately differentiated, 0/10 LN, 4.5 cm, +LV/PN invasion, +large vessel invasion; had been treated with adjuvant

gemcitabine and radiation therapy. Patient 4: T3N1 ductal adenocarcinoma with G12V mutant KRAS, well differentiated, 1/14 LN, +LV/PN invasion, unable to identify grossly; had been treated with adjuvant gemcitabine. Freshly resected tumors were subcutaneously implanted in NSG mice as previously described (22) and randomized into vehicle control (4–6 mice) or FGTI-2734 (5–7 mice) groups for each of the PDXs. Mice implanted with PDXs from patients 1, 2, and 3 were treated with 100 mg/kg body weight/day FGTI-2734. PDX from patient 4 and a separate PDX from patient 3 were treated with 50 mg/kg body weight/day FGTI-2734. Throughout treatment, FGTI-2734 at 50 or 100 mg/kg body weight significantly inhibited tumor growth of all 4 PDXs (Fig. 4, right panel, and Supplementary Fig. 2). By the last day of vehicle treatment, PDXs from patients 1, 2, and 3 showed average growth of 253%, 640%, and 411%, respectively. In contrast, FGTI-2734 treatment resulted in only 92%, 236%, and 136% growth, respectively (Fig. 4, right panel). Differences in tumor growth between vehicle- and FGTI-2734-treated mice were statistically significant ($P<0.05$) starting at day 2 (patients 1 and 2) and day 3 (patient 3) (Fig. 4, right panel). At 50 mg/kg body weight/day, FGTI-2734 also significantly inhibited patient 3 and 4 PDX growth, although less effectively than at 100 mg/kg body weight/day (Supplementary Fig. 2).

FGTI-2734 suppresses oncogenic signaling pathways mediated by AKT, mTOR, and cMYC while upregulating the tumor suppressor p53 and inducing apoptosis in patient-derived xenografts in vivo

We next investigated the effects of FGTI-2734 in vivo on the canonical RAS signaling pathways and other tumor survival pathways in patient-derived tumors. To this end, freshly resected tumors from patient 2 were subcutaneously implanted in 13 NSG mice, which were then randomized for daily 21-day treatment with vehicle (6 mice) or 100 mg/kg body weight FGTI-2734 (7 mice). Two hours after the last treatment, tumors were harvested and lysates were processed for Western blotting. As shown in Fig. 5A, FGTI-2734 inhibited the farnesylation of HDJ2 and the geranylgeranylation of RAP1A. Furthermore, FGTI-2734 suppressed P-AKT and P-S6 levels, suggesting that FGTI-2734 significantly affected the PI3K/AKT/mTOR signaling pathway. Data quantification showed that, on average, P-AKT/AKT and P-S6/S6 levels were inhibited by 75 ± 4% ($P=0.00005$) and 82 ± 15% ($P=0.003$), respectively (Fig. 5B). In contrast, FGTI-2734 minimally affected the other Ras canonical Raf/Mek/Erk pathway. Indeed, P-Erk1–2/Erk1–2 was only inhibited by 18 ± 6% ($P=0.04$) (Fig. 5B). FGTI-2734 suppressed the levels of the oncogene cMYC while upregulating the levels of the pro-apoptotic tumor suppressor p53 and in parallel induced CASPASE 3 activation (Fig. 5A). FGTI-2734 inhibited cMYC/β-ACTIN levels by 71 ± 4% ($P=0.0006$) (Fig. 5B) and induced p53/β-ACTIN and CASPASE 3/β-ACTIN levels by 2.9 ± 0.6-fold ($P=0.027$) and 1.71 ± 0.04-fold ($P=0.001$), respectively (Fig. 5C).

FGTI-2734 as a single agent is lethal to low-passage primary and metastatic mutant KRAS adenocarcinoma cells derived from pancreatic cancer patients

Using previously described methods (23, 24), we generated low-passage (<20) human pancreatic cancer cells to evaluate the lethality of FGTI-2734 in standard and three-dimensional culture systems. These lines were derived from primary and metastatic human tumors from 8 pancreatic cancer patients, in which previously performed sequencing (25) identified point mutations in codons 12 and 13 in all of the cell lines (Table 1). When the 8

patient-derived tumor cell lines were treated with FGTI-2734 in 2 dimensional standard conditions, we observed a dose-dependent inhibition of viability (Fig. 6, A and B), with IC50 values ranging between 6 and 28 μM (Table 1). Importantly, FGTI-2734 was more potent, with IC50 values between 5 and 9 μM, when the patient-derived tumor cells were cultured in three-dimensional conditions alone or when co-cultured with the chemoresistance-promoting human pancreatic stellate cells harvested from pancreatic adenocarcinoma cells (Fig. 6, C and D).

Discussion

Patients with mutant KRAS tumors suffer from poor prognosis, increased tumor aggressiveness and metastasis, and are less likely to respond to chemotherapy and targeted therapies (4–7, 14, 15). Most affected are pancreatic cancer patients with pancreatic adenocarcinoma where the mt KRAS prevalence is 90 % (14). Although recent studies have reported on small molecules that are capable of targeting KRAS (3, 10–12), so far no approved KRAS therapies are available in the clinic (3, 8–12). Attempts to target these cancers by blocking KRAS farnesylation have been unsuccessful in clinic, at least in part due to geranylgeranylation of KRAS by GGT-1 under FTI pressure (13). Here, we designed a dual FT and GGT1 inhibitor, FGTI-2734, which can prevent, unlike the selective FTI-2148 and GGTI-2418 inhibitors, membrane localization of KRAS, hence solving this major KRAS resistance problem. Our pharmacological and genetic approaches show that cytosolic KRAS is still able to bind one of its major effectors RAF-1 but is not able to activate it, possibly due to inhibition of binding to the scaffolding protein KSR (see Figure 2B) which plays a major role in RAS activation of Raf (26). The observation that cytosolic KRAS is able to bind but not to activate RAF-1 is consistent with our earlier report with the exclusively farnesylated HRAS, where we showed that treatment of mutant HRAS expressing NIH3T3 cells with the selective FT inhibitor, FTI-277, resulted in the accumulation of inactive cytoplasmic HRAS-Raf complexes (27).

An important finding of our study is that, although FGTI-2734 inhibited KRAS membrane association in all 6 human cancer cell lines that harbor mutant KRAS, it only induced apoptosis and inhibited tumor growth in mice with tumors in which CRISPR/Cas9/gRNA-targeted knockout of KRAS induced apoptosis (MiaPaCa2, Calu6, and L3.6pl) but not in cells where KRAS knockout did not induce apoptosis (A549, H460, and DLD1). The demonstration that FGTI-2734 is efficacious at selectively inhibiting growth in mutant KRAS-dependent versus mutant KRAS-independent tumors and at doses that were not toxic to mice underscores the specificity of FGTI-2734. Consistent with its specificity and lack of toxicity in our in vivo investigations, we also found that FGTI-2734 did not induce apoptosis in normal cells and in human cancer cells with wild-type RAS.

The fact that not all human tumors that harbor mutant KRAS are dependent on KRAS, coupled with the demonstration that FGTI-2734 is efficacious in only those that depend on mutant KRAS, suggests that cancers such as pancreatic cancer, which is known to be driven by mutant KRAS, may be responsive to FGTI-2734 treatment. Consistent with this, FGTI-2734 inhibited the in vivo growth of PDXs from 4 patients with pancreatic cancer. The FGTI-2734 anti-tumor activity shown in PDXs from patients with aggressive tumors that

were refractory to chemotherapy underscores its potential in overcoming tumor resistance. These anti-tumor effects were independent of the mutant KRAS isoforms, which varied from G12C, G12D, and Q61K (cell lines) to G12D, G12V, and G13D (patients). This is an important finding, as the position and the type of mutations in KRAS are thought to influence its transforming capacity, as well as drug response, in cancer patients.

In addition to its in vivo antitumor activity against PDXs, FGTI-2734 was also efficacious at inhibiting the viability of early-passage mutant KRAS-driven cancer cells derived from pancreatic cancer patients. This is an important finding, as we have previously demonstrated that early-passage mutant KRAS-driven cancer cells derived from pancreatic cancer patients are generally resistant to chemotherapeutic agents, such as gemcitabine, with IC50 values over 100 μM (23). Importantly, as a single agent, FGTI-2734 was significantly more potent when patient-derived pancreatic tumor cells were co-cultured in a three-dimensional environment with pancreatic stellate cells. This is an important finding as pancreatic stellate cells are known to promote chemotherapeutic resistance through cross-talk with pancreatic cancer cells (28).

We found that FGTI-2734 effectively inhibited KRAS membrane localization and growth of mutant KRAS-dependent tumors at non-toxic doses. This is in contrast to Lobell et al (29), in which KRAS prenylation could not be inhibited without toxicity using L-778123, an inhibitor of both enzymes but with 50-fold selectivity for FT over GGT-1 (unlike FGTI-2734, which is an equipotent dual FT and GGT-1 inhibitor). Furthermore, our results are consistent with knockout mouse studies where simultaneous suppression of FT and GGT-1 was highly effective at preventing mutant KRAS-induced lung tumors and at improving mouse survival without toxicity (30). Thus, these genetic studies are consistent with our pharmacological findings and together warrant further development of dual FT and GGT1 inhibitors as safe therapeutics for cancer treatment.

Our findings may also have major implications for patients whose tumors harbor NRAS mutations. Indeed, NRAS is found mutated frequently in a number of cancers, including hematological malignancies, sarcomas, and melanomas; like KRAS, NRAS is also alternatively geranylgeranylated when cancer cells are treated with FTIs (13). FGTI-2734, but not FTI-2148 or GGTI-2418, inhibited NRAS membrane localization, suggesting that FGTI-2734 may be efficacious in the treatment of cancer patients whose tumors are driven by mutant NRAS.

Another important finding is that FGTI-2734 abrogated major signal transduction pathways downstream of KRAS that are known to be pivotal to survival and therapy resistance in a large number of human cancers. Indeed, treatment of PDX mice with FGTI-2734 suppressed the phosphorylation of AKT and S6, indicating that the activation of the PI3K/AKT/mTOR oncogenic pathway was thwarted by FGTI-2734 treatment. In contrast, Erk1/2, another major canonical pathway downstream of KRAS, was minimally affected, suggesting a non-promiscuous effect of FGTI-2734 on signaling pathways. FGTI-2734 also suppressed cMYC levels, increased p53 levels, and activated CASPASE 3, suggesting that the ability of FGTI-2734 to inhibit tumor growth could be due at least in part to the suppression of oncogenic pathways such as PI3K/AKT/mTOR and cMYC and the upregulation of tumor

suppressor pathways such as those mediated by the upregulation of p53. The ability of FGTI-2734 to prevent mutant KRAS from localizing to the membrane and inhibiting it from signaling downstream could explain the observed abrogation of the PI3K/AKT/mTOR pathway downstream of KRAS. However, considering that FGTI-2734 inhibits FT and GGT-1, enzymes that have many substrates[13], the inhibition of other farnesylated and/or geranylgeranylated proteins could also contribute to the FGTI-2734 effects on signaling, induction of apoptosis, and inhibition of tumor growth.

Finally, FGTI-2734 may be efficacious in a wide spectrum of human tumors, as pathways mediated by PI3K/AKT/mTOR, cMYC, and p53 mediate oncogenesis in most human cancers. For example, in a recent study of 19,784 tumor samples representing over 40 cancer types, 38% of patients had an alteration in 1 or more PI3K/AKT/mTOR pathway component, most commonly PTEN loss and mutations in PIK3CA, PTEN, or AKT1 (31). Importantly, activation of the PI3K/AKT/mTOR pathway is associated with poor patient survival (32). Furthermore, p53 is either deleted or mutated in about 50% of human cancers or inactivated/down-regulated in the other 50% (33). Finally, cMYC overexpression through gene amplification is also common in human cancers, including pancreatic (14%), breast (27%), ovarian (31%), colorectal (6%), lung (5%), and renal cell carcinoma (23%) (34).

Taken together, we have designed FGTI-2734, a dual FT and GGT-1 inhibitor capable of suppressing major cancer-causing pathways, upregulating the tumor suppressor p53, and activating CASPASE 3, leading to thwarted growth in vivo and in vitro of patient-derived tumors from 12 pancreatic cancer patients with different KRAS mutations. Further preclinical studies are warranted to support the clinical development of FGTI-2734 in tumors where mutant KRAS is a major contributor to their malignancy and resistance to therapy.

Supplementary Material

Refer to Web version on PubMed Central for supplementary material.

Acknowledgements

This work was funded in part by NIH grant R35 CA197731–01 (Said Sebti, PhD) and was supported in part by the Chemical Biology, Molecular Genomics and SAIL Core Facilities at the H. Lee Moffitt Cancer Center & Research Institute; an NCI-designated Comprehensive Cancer Center (P30-CA076292). We thank these cores for their outstanding assistance and expertise. Part of the work was also supported in part by MD Anderson Cancer Center P30-CA016672. We also thank Michelle Blaskovich for technical assistance, and Rasa Hamilton for editorial assistance. Synthesis of some of the compounds reported in this publication was supported by NIH grant R50CA211447 (Harshani R. Lawrence).

References

1. Hanahan D, Weinberg RA. Hallmarks of cancer: the next generation. Cell 2011;144(5):646–74. [PubMed: 21376230]
2. Pylayeva-Gupta Y, Grabocka E, Bar-Sagi D. RAS oncogenes: weaving a tumorigenic web. Nat Rev Cancer 2011;11(11):761–74. [PubMed: 21993244]
3. Simanshu DK, Nissley DV, McCormick F. RAS Proteins and Their Regulators in Human Disease. Cell 2017;170(1):17–33. [PubMed: 28666118]

4. Chetty R, Govender D. Gene of the month: KRAS. J Clin Pathol 2013;66(7):548–50. [PubMed: 23626007]
5. Lievre A, Bachet JB, Le Corre D, Boige V, Landi B, Emile JF, et al. KRAS mutation status is predictive of response to cetuximab therapy in colorectal cancer. Cancer Res 2006;66(8):3992–5. [PubMed: 16618717]
6. Pao W, Wang TY, Riely GJ, Miller VA, Pan Q, Ladanyi M, et al. KRAS mutations and primary resistance of lung adenocarcinomas to gefitinib or erlotinib. PLoS Med 2005;2(1):e17. [PubMed: 15696205]
7. Slebos RJ, Kibbelaar RE, Dalesio O, Kooistra A, Stam J, Meijer CJ, et al. K-ras oncogene activation as a prognostic marker in adenocarcinoma of the lung. N Engl J Med 1990;323(9):561–5. [PubMed: 2199829]
8. Cox AD, Fesik SW, Kimmelman AC, Luo J, Der CJ. Drugging the undruggable RAS: Mission possible? Nat Rev Drug Discov 2014;13(11):828–51. [PubMed: 25323927]
9. Downward J RAS Synthetic Lethal Screens Revisited: Still Seeking the Elusive Prize? Clin Cancer Res 2015;21(8):1802–9. [PubMed: 25878361]
10. McCormick F Targeting KRAS Directly. Annual Review of Cancer Biology 2018;2(1):81–90.
11. Ostrem JM, Shokat KM. Direct small-molecule inhibitors of KRAS: from structural insights to mechanism-based design. Nat Rev Drug Discov 2016;15(11):771–85. [PubMed: 27469033]
12. Welsch ME, Kaplan A, Chambers JM, Stokes ME, Bos PH, Zask A, et al. Multivalent Small-Molecule Pan-RAS Inhibitors. Cell 2017;168(5):878–89 e29. [PubMed: 28235199]
13. Berndt N, Hamilton AD, Sebti SM. Targeting protein prenylation for cancer therapy. Nat Rev Cancer 2011;11(11):775–91. [PubMed: 22020205]
14. Ma J, Jemal A. The rise and fall of cancer mortality in the USA: why does pancreatic cancer not follow the trend? Future Oncol 2013;9(7):917–9. [PubMed: 23837751]
15. Ma J, Siegel R, Jemal A. Pancreatic cancer death rates by race among US men and women, 1970–2009. J Natl Cancer Inst 2013;105(22):1694–700. [PubMed: 24203988]
16. Peng H, Carrico D, Thai V, Blaskovich M, Bucher C, Pusateri EE, et al. Synthesis and evaluation of potent, highly-selective, 3-aryl-piperazinone inhibitors of protein geranylgeranyltransferase-I. Org Biomol Chem 2006;4(9):1768–84. [PubMed: 16633570]
17. Sun J, Blaskovich MA, Knowles D, Qian Y, Ohkanda J, Bailey RD, et al. Antitumor efficacy of a novel class of non-thiol-containing peptidomimetic inhibitors of farnesyltransferase and geranylgeranyltransferase I: combination therapy with the cytotoxic agents cisplatin, Taxol, and gemcitabine. Cancer Res 1999;59(19):4919–26. [PubMed: 10519405]
18. Prior IA, Hancock JF. Ras trafficking, localization and compartmentalized signalling. Semin Cell Dev Biol 2012;23(2):145–53. [PubMed: 21924373]
19. Kazi A, Xiang S, Yang H, Delitto D, Trevino J, Jiang RHY, et al. GSK3 suppression upregulates beta-catenin and c-Myc to abrogate KRas-dependent tumors. Nat Commun 2018;9(1):5154. [PubMed: 30514931]
20. Fleming JB, Shen GL, Holloway SE, Davis M, Brekken RA. Molecular consequences of silencing mutant K-ras in pancreatic cancer cells: justification for K-ras-directed therapy. Mol Cancer Res 2005;3(7):413–23. [PubMed: 16046552]
21. Singh A, Greninger P, Rhodes D, Koopman L, Violette S, Bardeesy N, et al. A gene expression signature associated with “K-Ras addiction” reveals regulators of EMT and tumor cell survival. Cancer Cell 2009;15(6):489–500. [PubMed: 19477428]
22. Delitto D, Pham K, Vlada AC, Sarosi GA, Thomas RM, Behrns KE, et al. Patient-derived xenograft models for pancreatic adenocarcinoma demonstrate retention of tumor morphology through incorporation of murine stromal elements. Am J Pathol 2015;185(5):1297–303. [PubMed: 25770474]
23. Kang Y, Zhang R, Suzuki R, Li SQ, Roife D, Truty MJ, et al. Two-dimensional culture of human pancreatic adenocarcinoma cells results in an irreversible transition from epithelial to mesenchymal phenotype. Lab Invest 2015;95(2):207–22. [PubMed: 25485535]
24. Kim MP, Evans DB, Wang H, Abbruzzese JL, Fleming JB, Gallick GE. Generation of orthotopic and heterotopic human pancreatic cancer xenografts in immunodeficient mice. Nat Protoc 2009;4(11):1670–80. [PubMed: 19876027]

25. Koay EJ, Lee Y, Cristini V, Lowengrub JS, Kang Y, San Lucas FA, et al. A visually apparent and quantifiable CT imaging feature identifies biophysical subtypes of pancreatic ductal adenocarcinoma. Clin Cancer Res 2018.

26. Claperon A, Therrien M. KSR and CNK: two scaffolds regulating RAS-mediated RAF activation. Oncogene 2007;26(22):3143–58. [PubMed: 17496912]

27. Lerner EC, Qian Y, Blaskovich MA, Fossum RD, Vogt A, Sun J, et al. Ras CAAX peptidomimetic FTI-277 selectively blocks oncogenic Ras signaling by inducing cytoplasmic accumulation of inactive Ras-Raf complexes. J Biol Chem 1995;270(45):26802–6. [PubMed: 7592920]

28. Wu Q, Tian Y, Zhang J, Zhang H, Gu F, Lu Y, et al. Functions of pancreatic stellate cell-derived soluble factors in the microenvironment of pancreatic ductal carcinoma. Oncotarget 2017;8(60): 102721–38. [PubMed: 29254283]

29. Lobell RB, Liu D, Buser CA, Davide JP, DePuy E, Hamilton K, et al. Preclinical and clinical pharmacodynamic assessment of L-778,123, a dual inhibitor of farnesyl:protein transferase and geranylgeranyl:protein transferase type-I. Mol Cancer Ther 2002;1(9):747–58. [PubMed: 12479371]

30. Liu M, Sjogren AK, Karlsson C, Ibrahim MX, Andersson KM, Olofsson FJ, et al. Targeting the protein prenyltransferases efficiently reduces tumor development in mice with K-RAS-induced lung cancer. Proc Natl Acad Sci U S A 2010;107(14):6471–6. [PubMed: 20308544]

31. Millis SZ, Ikeda S, Reddy S, Gatalica Z, Kurzrock R. Landscape of Phosphatidylinositol-3-Kinase Pathway Alterations Across 19784 Diverse Solid Tumors. JAMA Oncol 2016;2(12):1565–73. [PubMed: 27388585]

32. Ocana A, Vera-Badillo F, Al-Mubarak M, Templeton AJ, Corrales-Sanchez V, Diez-Gonzalez L, et al. Activation of the PI3K/mTOR/AKT pathway and survival in solid tumors: systematic review and meta-analysis. PLoS One 2014;9(4):e95219. [PubMed: 24777052]

33. Kastenhuber ER, Lowe SW. Putting p53 in Context. Cell 2017;170(6):1062–78. [PubMed: 28886379]

34. Kalkat M, De Melo J, Hickman KA, Lourenco C, Redel C, Resetca D, et al. MYC Deregulation in Primary Human Cancers. Genes (Basel) 2017;8(6).

35. Fletcher S, Keaney EP, Cummings CG, Blaskovich MA, Hast MA, Glenn MP, et al. Structure-based design and synthesis of potent, ethylenediamine-based, mammalian farnesyltransferase inhibitors as anticancer agents. J Med Chem 2010;53(19):6867–88. [PubMed: 20822181]

36. van der Hoeven D, Cho KJ, Ma X, Chigurupati S, Parton RG, Hancock JF. Fendiline inhibits K-Ras plasma membrane localization and blocks K-Ras signal transmission. Mol Cell Biol 2013;33(2):237–51. [PubMed: 23129805]

Statement of Translational Relevance

Mutant KRAS drives pancreatic oncogenesis and therapy resistance, yet there are no drugs in the clinic to target mutant KRAS. Here we report on the development of a novel peptidomimetic dual farnesyl/geranylgeranyl transferase inhibitor (FGTI-2734) that thwarts mutant KRAS patient-derived pancreatic tumors. Although FTIs block membrane localization, a step required for RAS oncogenesis, KRAS becomes geranylgeranylated and FGTI-2734 overcomes this geranylgeranylation-dependent resistance. FGTI inhibits KRAS membrane localization in pancreatic, lung, and colon human cancer cells. FGTI was effective in patient-derived tumors from 12 pancreatic cancer patients with G12D, G12V and G13D KRAS primary and metastatic tumors. FGTI efficacy was demonstrated in relevant models including patient-derived xenografts and 3D co-cultures with resistance-promoting pancreatic stellate cells. Pharmacodynamic analysis in patient-derived xenografts showed that FGTI suppressed oncogenic pathways mediated by AKT, mTOR, and cMYC while upregulating p53. This discovery opens new avenues to target mutant KRAS-driven cancers, and as such it warrants further advanced preclinical and clinical studies.

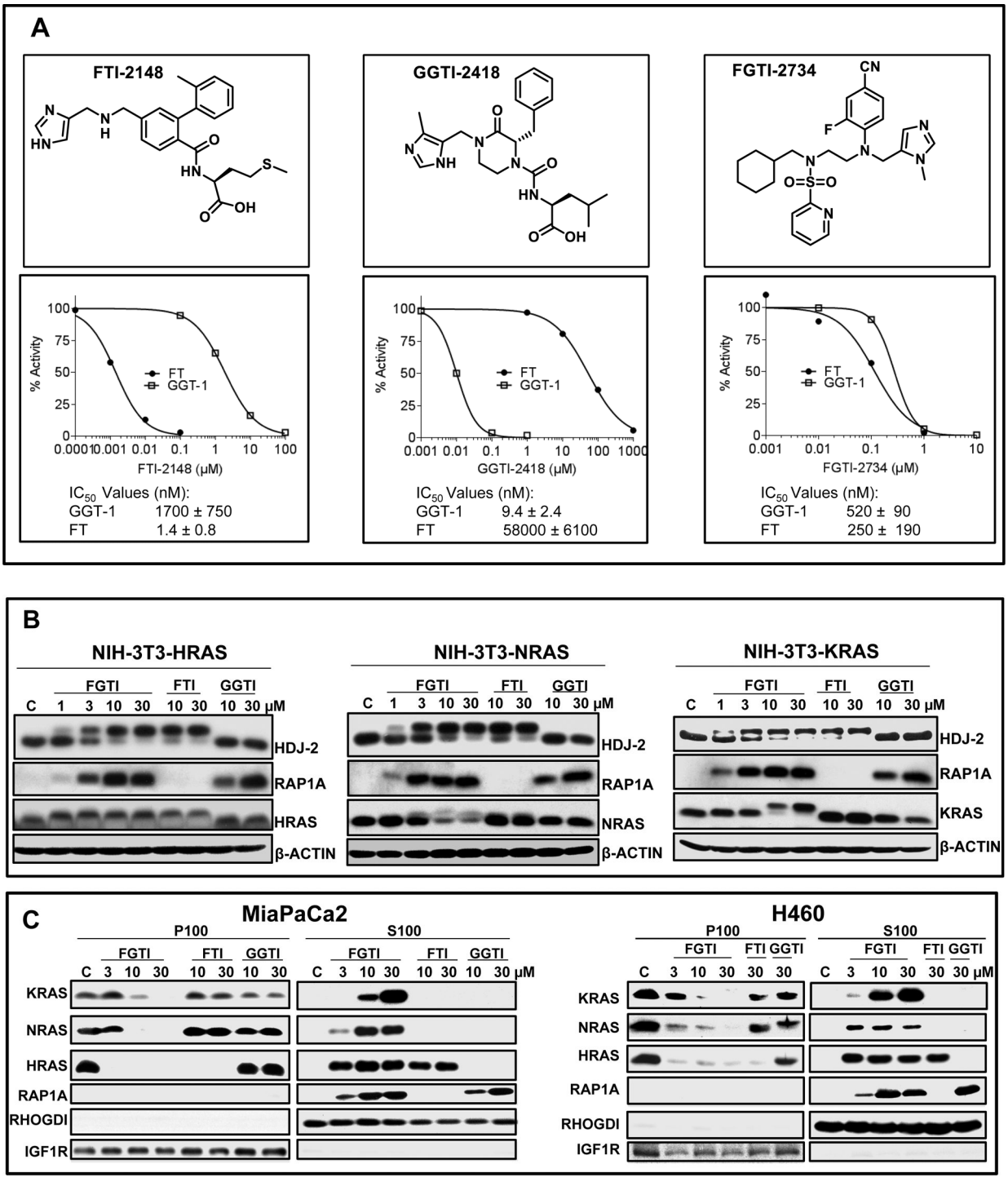

Figure 1. FGTI-2734, but not FTI-2148 or GGTI-2418, inhibits both protein prenylation and membrane localization of KRAS and NRAS.

A, Chemical structures and in vitro potency and selectivity of FTI-2148, GGTI-2418, and FGTI-2734. **B**, KRAS HRAS, and NRAS-transformed NIH3T3 cells were treated with vehicle (DMSO) or various concentrations of FGTI-2734, FTI-2148, and GGTI-2418 and processed for Western blotting with antibodies to KRAS, HRAS, NRAS, HDJ2, and

RAP1A. Unprenylated bands of HDJ2, KRAS, HRAS, and NRAS show slower migration compared with fully prenylated HDJ2, KRAS, HRAS, and NRAS. RAP1A antibody can detect only unprenylated RAP1A. **C**, Human pancreatic cancer MiaPaCa2 and human lung cancer H460 cells were treated with vehicle (DMSO) or various concentrations of FGTI-2734, FTI-2148, and GGTI-2418, processed for membrane (P100) and cytosolic (S100) fractionation, and analyzed with Western blot using antibodies to KRAS, HRAS NRAS, and RAP1A. RHOGDI and IGF1R antibodies were used for internal controls for cytosolic and membrane fractions, respectively.

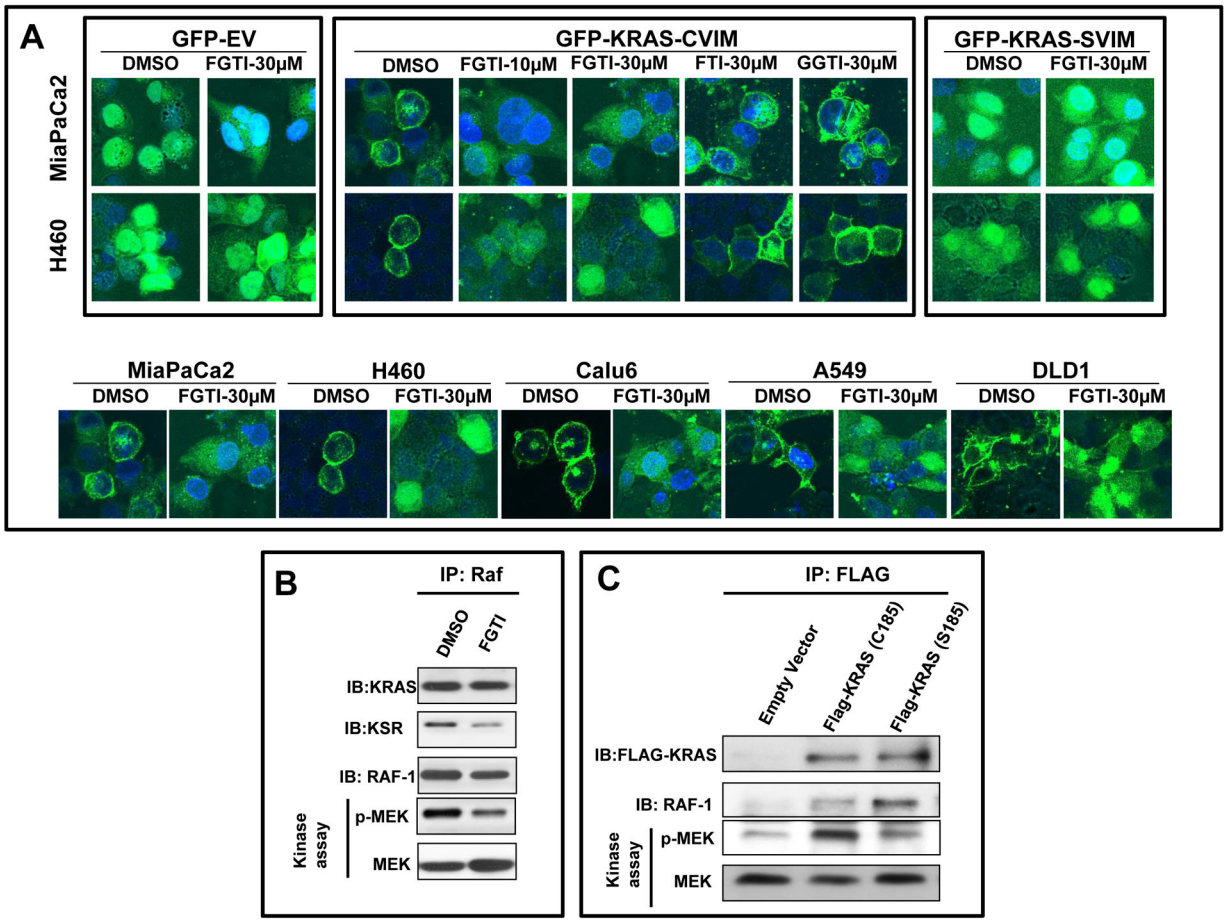

Figure 2. Effects of accumulating KRAS in the cytosol on binding to RAF-1 and KSR and on RAF-1 kinase activity.

A, FGTI-2734, but not FTI-2148 or GGTI-2418, inhibits membrane localization of GFP mutant KRAS-CVIM in human cancer cells. MiaPaCa2, H460, Calu6, A549, and DLD1 cells were grown on glass coverslips and infected with lentiviruses of GFP-tagged mutant KRAS-CVIM, GFP-tagged 185 Cys to Ser mutant KRAS that cannot be prenylated (GFP-mutant KRAS-SVIM), and corresponding empty vector (GFP-tagged-EV) and treated with vehicle control (DMSO) or FGTI-2734, FTI-2148, or GGTI-2418. Cells were fixed and viewed through a confocal microscope. **B**, FGTI-2734 inhibits RAF-1 kinase activity and binding to KSR but not to KRAS. MiaPaCa2 cells were treated with FGTI-2734 at 30 μM and processed for RAF-1 immunoprecipitation, followed by KRAS and KSR immunoblotting as well as RAF-1 kinase assay in the immunoprecipitates using recombinant inactive MEK1 as a substrate and western blotting with an antibody to phosphorylated Serines 217 and 221as described under Methods. **C**, The cytosolic CAAX mutant KRASG12V-SVIM binds RAF-1 but does not activate it. MiaPaCa2 cells expressing FLAG-tagged KRASG12V-CVIM or FLAG-tagged KRASG12V-SVIM were processed for coimmunoprecipitation and RAF-1 kinase assays as described above.

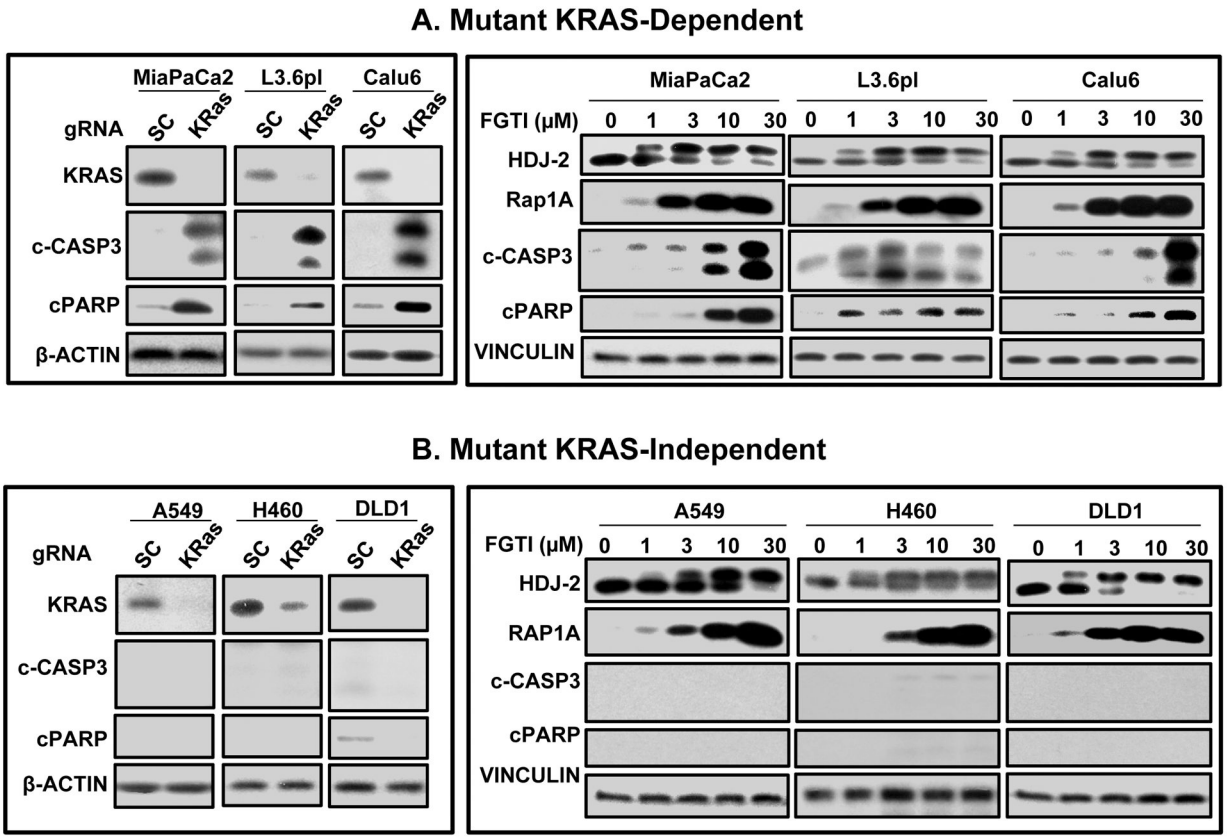

Figure 3. FGTI-2734 induces apoptosis in mutant KRAS-dependent, but not independent, human cancer cell lines with different oncogenic KRAS mutation.

A, mutant KRAS harboring MiaPaCa2, L3.6pl, and Calu6 (mutant KRAS-dependent cell lines). **B**, mutant KRAS harboring A549, H460, and DLD1 (mutant KRAS-independent cell lines). For both panels, cells were transiently infected with lentiviral guide RNAs (gRNA) of scrambled (SC) and KRAS gRNAs and treated with either vehicle (DMSO) or indicated concentrations of FGTI-2734 followed by Western blot analysis with indicated antibodies.

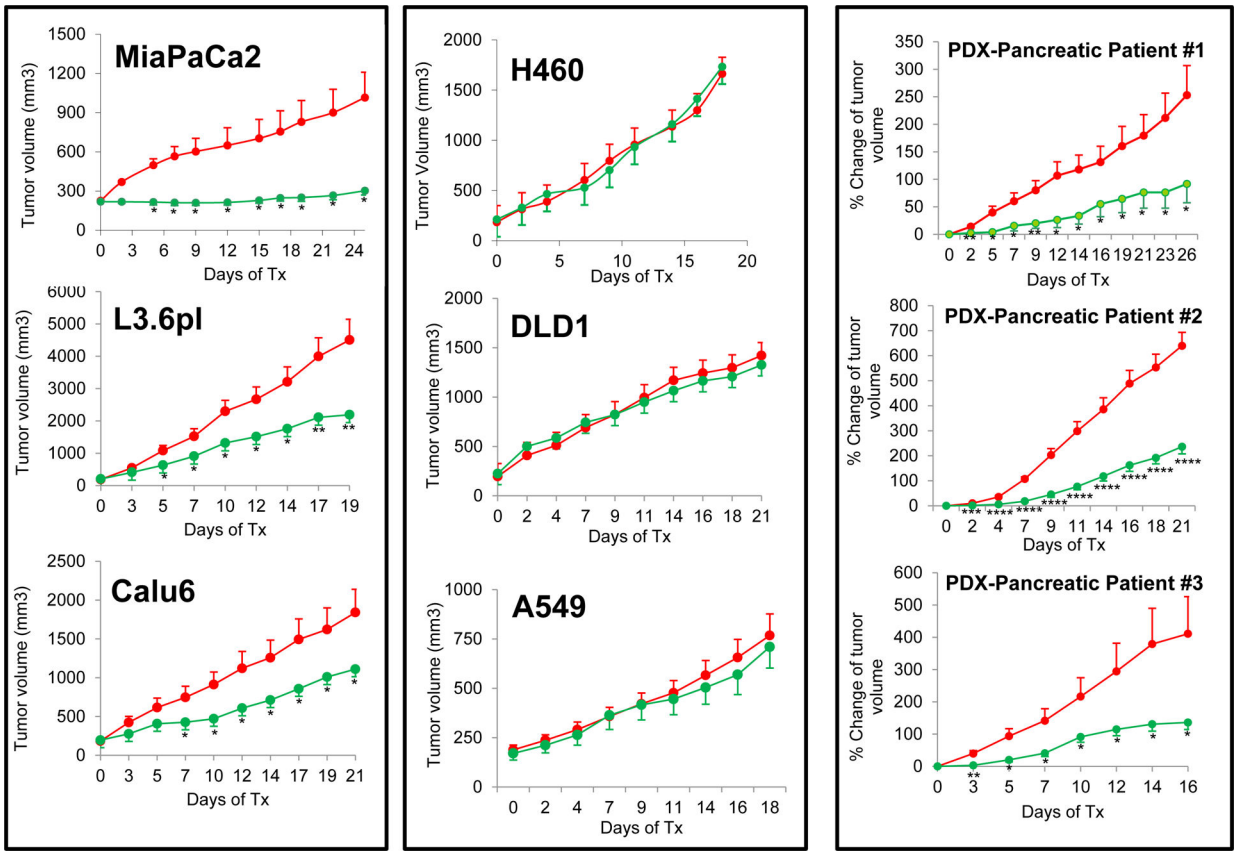

Figure 4. FGTI-2734 inhibits in vivo growth of mutant KRAS-dependent (MiaPaCa2, L3.6pl, Calu6), but not mutant KRAS-independent (A549, H460 and DLD1), tumors and inhibits growth of xenografts from pancreatic cancer patients.

The growth of human tumors following injection of MiaPaCa2, L3.6pl, Calu6 (left panels), A549, H460, and DLD1 (middle panels) cancer cells into SCID-bg mice was determined as described in the Methods. Mice were treated with vehicle (red) and 100 mg/kg body weight FGTI-2734 (green). Right panels show effects of vehicle (red) and 100 mg/kg body weight FGTI-2734 (green) on growth of patient-derived xenograft (PDXs) tumors from patients with pancreatic cancer. Data are presented as means ± standard error. Asterisks indicate statistical significance ($p < 0.05$).

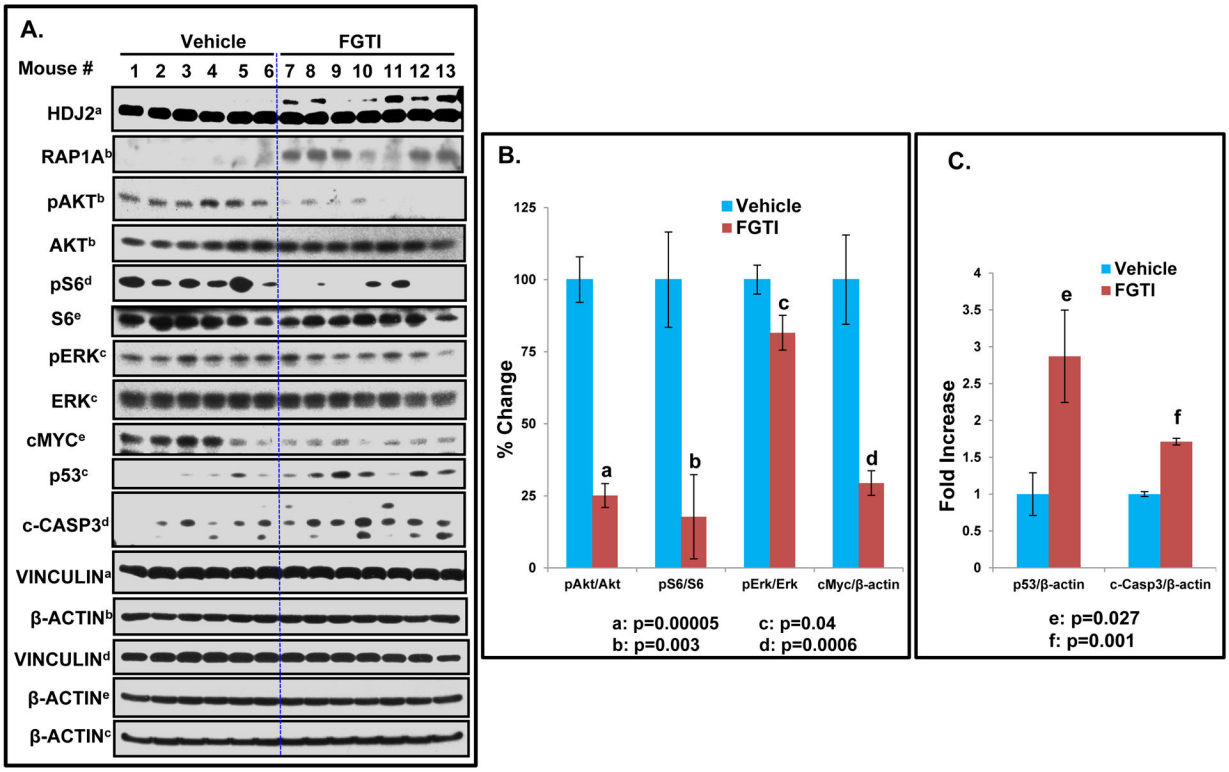

Figure 5. FGTI-2734 inhibits oncogenic pathways mediated by AKT, mTOR, and cMYC, upregulates the tumor suppressor p53, and activates CASPASE 3 in patient-derived xenografts in vivo.

Tumor tissue lysates from 6 vehicle-treated (mouse 1–6) and 7 FGTI-2734-treated (100mg/kg body weight; mouse 7–13) mice from patient 2 PDX were processed for Western blot analysis with indicated antibodies. **A**, Western blot results; superscripts a-e shown by antibodies correspond to loading controls containing vinculin or β-ACTIN. **B and C**, Quantification of Western blot results; letters a-f indicate statistical significance (P<0.05).

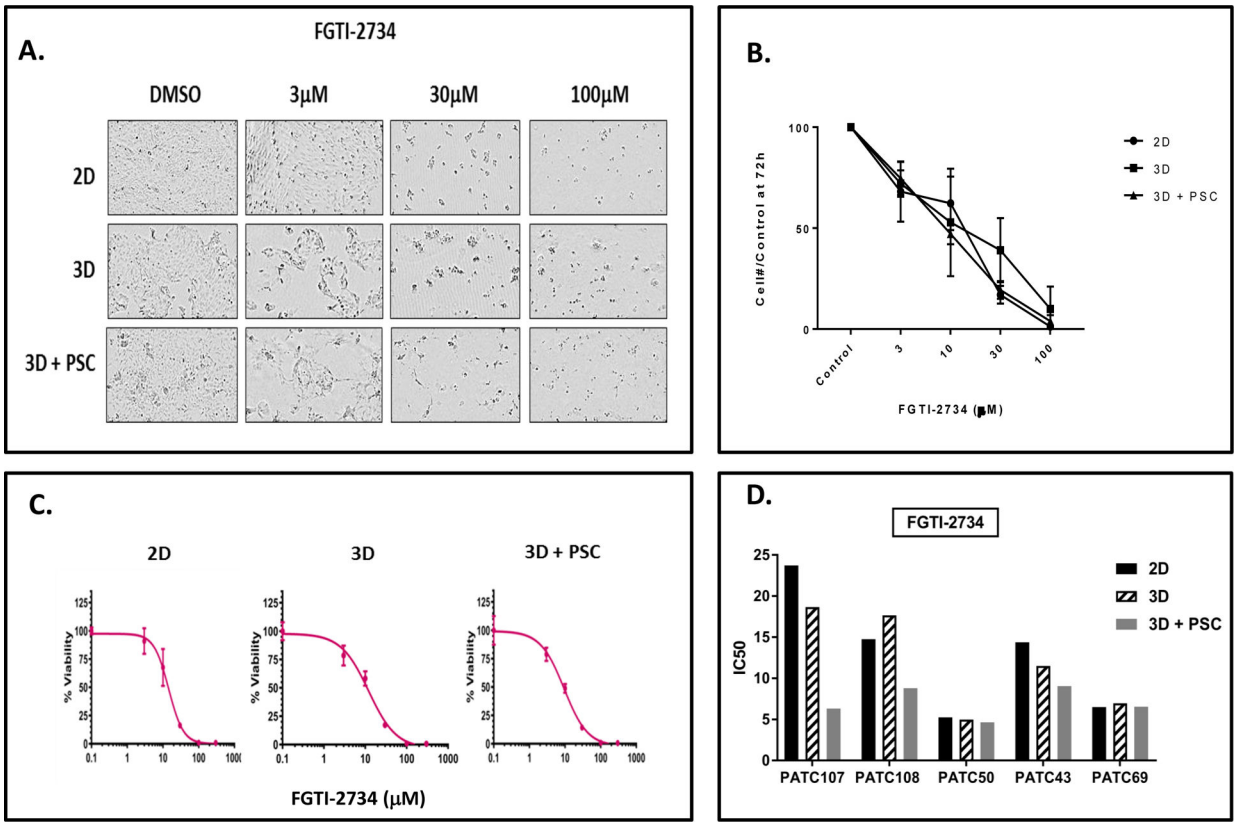

Figure 6. FGTI-2734 inhibits the viability, in 2-dimension, 3-dimension, and 3-dimension co-cultures with pancreatic stellate cells (PSCs) of low-passage primary and metastatic mutant KRAS adenocarcinoma cells derived from pancreatic cancer patients.

Cells derived from patients 107, 108, 50, 43 and 69 (please see Table 1 for more detail) were cultured as described in Methods and subsequently treated for 72 hours with indicated concentrations of FGTI-2734. **A, B, C cells were derived from patient # 43. A**, Live-cell imaging was carried out with the IncuCyte Zoom at 72 hours (representative image). **B**, Cell number was analyzed using IncuCyte software on day 0 and 72 hour posttreatment; day 0 was used as control. **C**, Cell viability was determined using the CellTiter-Glo luminescent cell viability assay (representative image). **D**, IC50 was determined for pancreatic cancer cells (derived from 5 patients) treated for 72 hours with FGTI-2734 using GraphPad Prism 7.02 software.

Table 1.

FGTI-2734 inhibits the viability of low passage primary and metastatic mutant KRAS adenocarcinoma cells derived from pancreatic cancer patients

Sample	Origin	KRAS	IC 50 (μM)
PATC107	Primary	p.Gly12Val	19.86
PATC108	Primary	p.Gly12Asp	15.78
PATC50	Primary	p.Gly12Val	6.54
PATC102	Primary	p.Gly13Asp	6.33
PATC148	Liver metastasis	p.Gly12Asp	28.85
PATC53	Liver metastasis	p.Gly12Asp	14.51
PATC43	Primary	p.Gly12Val	24.33
PATC66	Primary	p.Gly12Asp	16.38